Single-trial detection of realistic images with magnetoencephalography

Hubert Cecotti and Girijesh Prasad
Intelligent Systems Research Centre (ISRC), School of Computing and Intelligent Systems
Ulster University
Derry/Londonderry, Northern Ireland, UK
email: {h.cecotti,g.prasad}@ulster.ac.uk

***Abstract*—The detection of brain responses corresponding to the presentation of a particular class of images is a challenge in Brain-Machine Interface (BMI). Brain decoding is nowadays possible thanks to advanced brain recording devices (fMRI, EEG, MEG), and the use of appropriate signal processing and machine learning techniques. Current systems based on the detection of brain responses during rapid serial visual presentation (RSVP) tasks use EEG recording. We propose to evaluate the performance of single-trial detection with signal recorded with magnetoencephalography (MEG) during an RSVP task where participants were asked to detect images containing a person. We compare several classifiers (LDA, BLDA, k-nearest neighbor, support-vector machines) with spatial filtering, and with different sets of channels (magneto-meters, gradio-meters, all the channels). The results suggest that single-trial detection can be obtained with an AUC superior to 0.95, while typical studies based on EEG recordings using the same type of tasks, the AUC is often around 0.8. The present results show that MEG can be successfully used for target detection during a difficult RSVP task.**

I. Introduction

Magnetoencephalography (MEG) signal has several advantages over EEG signal. First , it allows to measure non-invasively the ongoing brain activity with sub-millisecond time resolution. Second, it is possible to obtain a high spatial resolution thanks to the 306 sensors that are distributed over the head. Therefore, it can be possible to localize in the brain with certain accuracy where the activity is produced. Thanks to those properties, MEG is well suited for studying the human brain dynamics and the different brain areas that are involved during various cognitive tasks [1]. While the main applications of MEG are related to clinical studies and neuroscience research, other potential applications can be possible in relation to what has been done during several decades with EEG in the field of Brain-Machine Interface (BMI). Like MEG, electroencephalography (EEG) has an excellent temporal resolution, but MEG has a more precise spatial resolution by mapping the magnetic sources in the brain.

The neuromagnetic fields of the brain are very small, and they are usually in the order of 50-500 fT (10-15 Tesla). The neurmagnetic fields that are originated from the brain correspond to the resulting current of a synaptic input to a neuron. In order to detect the magnetic field outside the skull, it is necessary that a large population of neurons receives synaptic inputs within a short time-window. MEG is based on superconducting quantum interference device (SQUID) technology that was originally introduced in the 1960s. Current MEG systems contain a large number of SQUIDs connected to sensor coils in a helmet-like configuration. The MEG system must be placed in a magnetic shielded room due to the environmental magnetic noise that is higher than the magnetic fields coming from the head of a subject. Contrary to EEG recording where the cap is placed on a precise location on the head with an international system for the placement of the electrodes, the subject in an MEG system does not have his head against precise sensors. However, several sensors are placed on the head of the subject to readjust the recorded MEG signal to a normalized position. For instance, transformation of MEG signals between different head positions can be performed with Signal Space Separation (SSS) method.

Brain decoding is a popular research field as it aims at decoding the information in the brain [2], [3], [4]. Several types of tasks can be achieved: classification, identification, and reconstruction. Let us consider a set of N different stimuli $\{x_1, \dots, x_N\}$ with their respective labels coded as a number $\{y_1, \dots, y_N\}$, and s_i the recorded brain activity corresponding to the presentation of x_i, $1 \leq i \leq N$. Classification tasks aim at determining a function F_c, such that $F_c(s_i) = y_i$. The function F_d corresponding to an identification task can be defined by $F_d(s_i, \{x_1, \dots, x_k\}) = x_i$, where $\{x_1, \dots, x_k\}$ is a subset of stimuli, with $k \leq N$. In reconstruction, the purpose is to find a function F_r, such that $F_r(s_i) = x_i$. Such a task includes visual image reconstruction from human brain activity [5]. In this paper, we will consider a binary classification task.

The stability of the spatial distribution, the amplitude, and the latency of a brain evoked response are the key elements that allow robust single-trial detection. Thanks to signal processing methods that can denoise the signal and enhance its main discriminant characteristics, and advanced machine learning techniques, it is possible to detect brain evoked responses. This principle has been used in BMI to detect specific event-related potentials [6]. Several research groups have developed BMI virtual keyboards that are based on the detection of the ERP components such as the P300 [7] and the N200 [8]. Despite the stability of these ERP components, accurate and reliable detection of the specific neural responses often requires averaging multiple responses. For instance, it is common that about ten trials are averaged in BMI virtual keyboards to optimize the accuracy [9]. The requirements of several trials is mainly due to the noise in the EEG that is not task-related, and by the spatially diffuse distribution of the brain responses across sensors. Although averaging the signal from multiple brain responses can increase the efficiency of detection, it also decreases the information transfer rate of the BMI due to the number of trials that are needed to reach a robust decision [10]. Moreover, there exist tasks where it is not possible to repeat the visual stimuli: they appear only one time [11]. It happens when a subject watches a video. Each frame of the video is presented only one time. Thanks to the high spatial resolution of MEG, it is expected to achieve high performance in single-trial detection.

One application that has gained attention in the past decade has been single-trial target detection in rapid serial visual presentation (RSVP) tasks [12], [13]. In the RSVP paradigm, a rapid sequence of images are presented sequentially to subjects in the same location on a screen [14], [15]. The stream of images contains different types of visual stimuli, which can be classified as targets or non-targets. In relation to the task given to the object, *i.e.,* increment an imaginary variable each time an image corresponding to a particular class is presented, different brain responses will be evoked. This paradigm has been successfully used during visual search (*e.g.,* the triage of satellite images [16], [17], [18], [19], [20], face recognition tasks [21]). The main advantage of the RSVP task is that the speed of the stimulus sequence combined with single-trial detection can provide a means to increase the information transfer rates in BMI systems. In a previous international competition (MLSP) [22] using an RSVP task with EEG recordings, the area under the receiver operating characteristic (ROC) curve (AUC) [23] of the best subjects reached only about 0.82. While this result is significantly above a random decision, the decision of several trials should be combined to obtain a perfect accuracy.

Working with high quality signals is critical for high performance in single-trial classification. The primary purpose of the present study is to investigate the performance of various classifiers, with the addition of spatial filtering, on the single-trial detection of brain responses recorded during a difficult RSVP task with MEG. Parra et al. [24] show the relevance of linear analysis methods for discriminating between different events in single-trial. Other efficient strategies without spatial filtering have been proposed for EEG single-trial detection that can be also used for MEG. The methods in the literature include linear classifiers (Fisher's linear discriminant analysis), Bayesian Linear Discriminant Analysis [25], [26], support vector machines (SVM) [9], and artificial neural networks [27], [28]. The remainder of the paper is organized as follows. First, we present the experimental protocol. Second, we describe the signal processing and classification methods. Finally, the results are presented and discussed in the last two sections.

II. Methods

A. Subjects

Three volunteer healthy male subjects participated to the study (mean=30 sd=5.2). All participants provided written informed consent, reported normal or corrected-to-normal vision, and no history of neurological problems. All participants had no experience with MEG recordings. Only one subject had prior experience with the task.

B. Visual stimuli

Visual stimuli consisted of 300 color images (256×256 pixel). These images were taken from "Insurgency: Modern Infantry Combat" (Insurgency Team), a total conversion modification of the video game "Half-Life 2" (Valve corporation) that is available on Steam®. The realistic images were separated into target scenes that contained a person (100 images) and non-target scenes that did not contain a person (200 images). Figure 1 depicts several examples of the images that were presented during the experiments. The images were presented on a screen with a resolution of 1920×1080 pixels and a refresh rate of 60 Hz. The images were centered on the screen (visual angle $\approx 20^o$). Participants were seated comfortably 100 cm from the screen in a darkened electromagnetically shielded chamber.

Fig. 1. Examples of visual stimuli (**targets** (top) vs. **non-target** (bottom)).

C. Procedure and design

The rapid serial visual presentation task had the following properties: the stimulus onset asynchrony was set to 250 ms, *i.e.,* the images were presented at 4 Hz. The inter-stimulus interval was set to 0 s, *i.e.,* there was no blank between two images. The target probability was set to 10% [29]. The set of images was shuffled in such a way that it was not possible to see an image two times in row. Moreover, an additional constraint was set to the stream of images: it was not possible to see consecutively two images corresponding to a target. The duration of the experiment was 16.66 minutes, which corresponds to the presentation of 4000 images (3600 non-targets, and 400 targets).

D. Signal acquisition

The data was recorded with an Elekta Neuromag 306-channel MEG system at the Intelligent Systems Research Centre (ISRC), Ulster University, Derry/Londonderry, UK. The signal was recorded with a sampling rate of 1 kHz using 204 planar gradio-meters and 102 magneto-meters, based on thin-film technology. The planar gradio-meters are mostly sensitive to fields arising from nearby sources, whereas the magneto-meters couple strongly also to distant sources, and therefore the system provides accurate information of both brain signals and the interference. EMG electrodes were placed close to the eye to monitor eye blinks. Five head position indicator (HPI) coils were placed on the head to monitor eye movement during the task.

E. Temporal and spatial filtering

A common first step in analyzing the MEG data is to pre-process the signal using the Neuromag sofware Maxfilter 2.2 that implements Signal-Space Separation (SSS). The SSS method idealizes magnetic multichannel signals by transforming them into device-independent idealized channels representing the measured data in uncorrelated form [30], [31], [32]. The method is a purely spatial method to transform electromagnetic multi-channel signals into uncorrelated basic components. It separates magnetic signals coming from within the brain from those coming from outside. This processing step is useful for removing noise, particularly using its temporal extension (tSSS), for detecting bad channels, for interpolated data after movement if continuous HPI was recorded, and for moving the data to a standard space that can be analyzed across subjects. After applying SSS on the recorded signal, the signal was downsampled to 125 Hz, and bandpass-filtered between 0.1 Hz and 41.66 Hz. A time segment of 640 ms (80 time points) was used to capture ERP components, such as the P300 and N200, can appear during the presentation of a target as expected by the experimental protocol.

The next step consisted of enhancing the relevant signal using the xDAWN spatial filtering approach [33], which was also used for sensor selection [34], [35], [36]. In this method, spatial filters are obtained through the Rayleigh quotient by maximizing the signal-to-signal plus noise ratio (SSNR) [37]. The signal corresponds to the information relative to the presentation of a target. The result of this process provides N_f spatial filters that are ranked in terms of their SSNR. The enhanced signal XU is composed of three terms: the ERP responses on a target class ($D_1 A_1$), a response common to all stimuli, *i.e.,* all targets (images with a person) and non-targets (images without a person) confound ($D_2 A_2$), and the residual noise (H), that are all filtered spatially with U.

$$XU = (D_1 A_1 + D_2 A_2 + H)U. \quad (1)$$

where $\{D_1, D_2\} \in \mathbb{R}^{N_t \times N_1}$ are two Toeplitz matrices, N_1 is the number of sampling points representing the target and superimposed evoked potentials (640 ms), and $H \in \mathbb{R}^{N_t \times N_s}$. The spatial filters U maximize the SSNR:

$$\text{SSNR}(U) = \text{argmax}_{\ U} \ \frac{\text{Tr}(U^T \hat{A}_1^T D_1^T D_1 \hat{A}_1 U)}{Tr(U^T X^T X U)} \quad (2)$$

where $\hat{A}_1$ represents the least mean square estimation of A_1:

$$\hat{A} = \begin{bmatrix} \hat{A}_1 \\ \hat{A}_2 \end{bmatrix} = ([D_1; D_2]^T [D_1; D_2])^{-1} [D_1; D_2]^T X \quad (3)$$

where $[D_1; D_2] \in \mathbb{R}^{N_t \times (N_1 + N_2)}$ is obtained by concatenation of D_1 and D_2, and Tr(.) denotes the trace operator.

F. Classification

For the classification we consider the two first best spatial filters ($N_f = 2$). For the binary classification of target versus non-target images, we have used: LDA, BLDA, k-nearest neighbors (k-nn), and SVM, with a 4-fold cross validation procedure. The performance of single-trial classification in the subsequent sections was assessed by the area under the ROC curve. We evaluate the performance for three conditions: (1) the use of all magneto-meters (102 channels), (2) all the gradio-meters (204 channels), and (3) all the 306 channels.

III. Results

A. Evoked responses

Before classification, the signal was checked with Brainstorm [38]. The amplitude fluctuations over time for all the sensors are presented in Figure 2 for both the gradio-meters and the magneto-meters. The spatial distribution for two key time points are depicted in Figure 4. At 200 ms, it is possible to observe a strong activity in the occipital area, while at 350 ms the activity is more important in the parietal region. Those results are coherent with results in the event-related potential literature with EEG studies [39].

B. Single-trial detection

The performance for single-trial detection is presented for each classifier and each subject in Table I, II, III, and IV. The best performance is obtained with the BLDA classifier, with a mean AUC=0.894 ± 0.043. The best subject has a mean AUC of 0.960. It is worth mentioning that this subject was also the subject who had experience with the RSVP task. Other subjects provided comments about the difficulty of the task, as it is difficult to focus for a long time. The information transfer rate (ITR) in bits per minute (bpm) is defined by ITR= $\frac{60}{T} \cdot \psi$ where ψ, the information transfer rate, in bits per symbol, is defined by:

$$\psi = \vartheta_0 - \vartheta_1 \quad (4)$$

$$\vartheta_0 = -\sum_{j=1}^{N_{out}} p(w_j) \cdot log_2(p(w_j)) \quad (5)$$

$$\vartheta_1 = -\sum_{i=1}^{N_{out}} \sum_{j=1}^{N_{out}} p(w_i) \cdot p(w_j|w_i) \cdot log_2(p(w_j|w_i)) \quad (6)$$

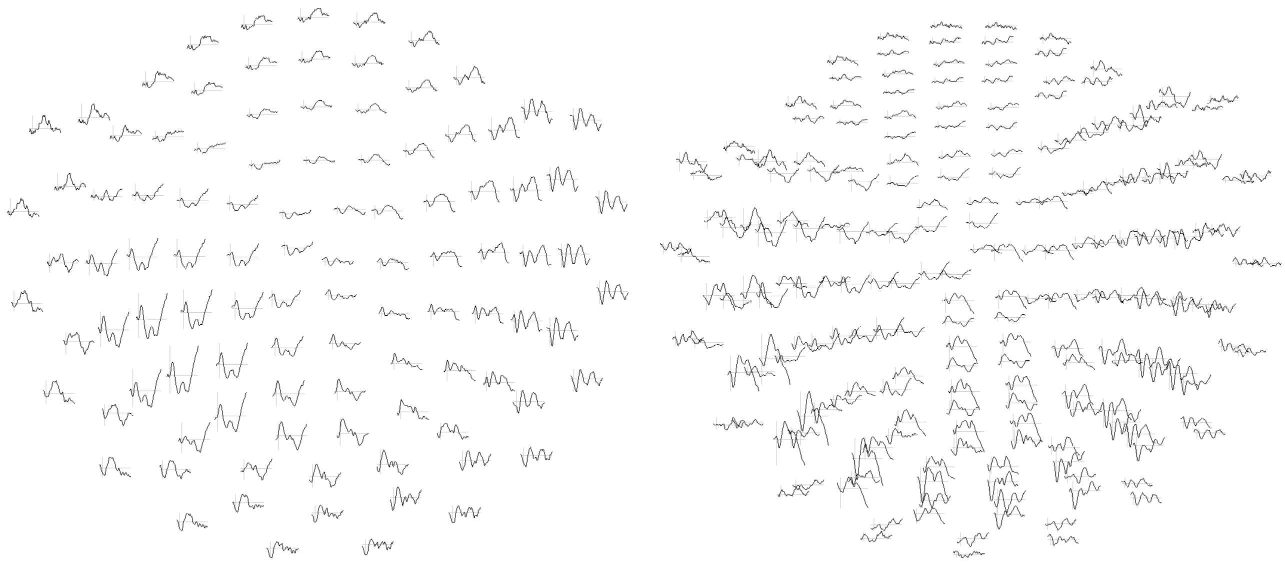

Fig. 2. Representation of the grand averaged difference between targets and non-target for both magneto-meters (**left**) and gradio-meters (**right**) for a representative subject (s1).

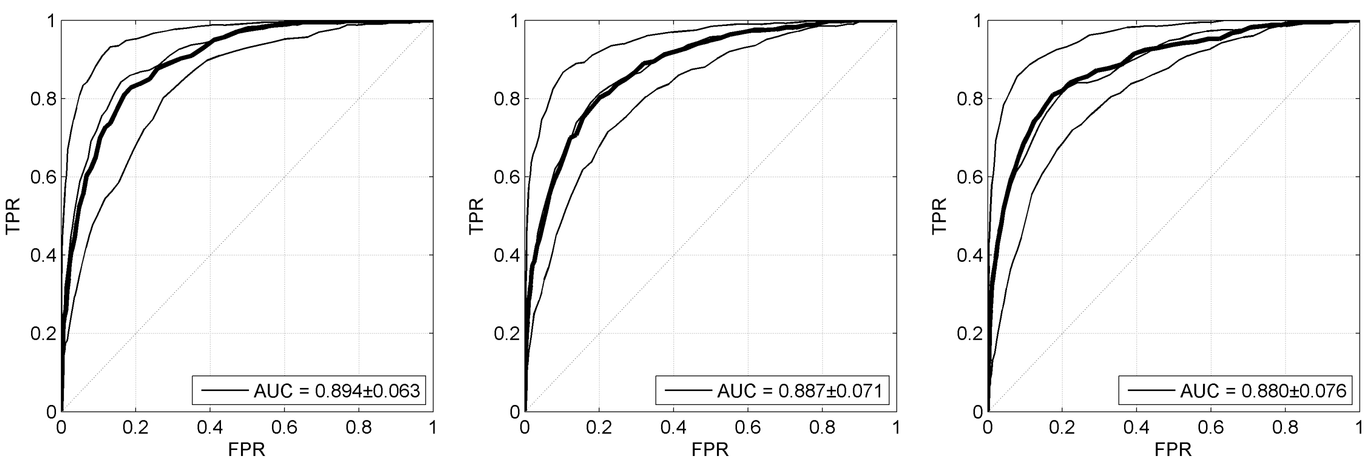

Fig. 3. ROC curve of the xDAWN+BLDA classification: magneto-meter channels (**left**), gradio-meter channels (**middle**), all channels (**right**). The bold curve represents an estimation of the mean AUC across subjects.

where N_{out} being the number of possible different outputs, and T being the time in seconds of recorded MEG signal that is required to take the decision among the N_{out} outputs. Due to the constraint of the target probability of 10%, we consider the Nykopp definition of the ITR, and $N_{out} = 2$ with $p(w_1) = 0.1$ and $p(w_2) = 0.9$ are the prior probabilities. $p(w_j|w_i)$ being the element (i, j) in the confusion matrix of the classification obtained with a threshold set to maximize the f-score in the training data-set. The ITR for the best subject reaches 0.46 bits/symbol, or 110 bits/minute.

TABLE I
AUC FOR XDAWN+BLDA CLASSIFICATION.

Subject	Mag	Grad	All
s1	0.960 ± 0.023	0.960 ± 0.022	0.957 ± 0.024
s2	0.887 ± 0.058	0.882 ± 0.062	0.877 ± 0.065
s3	0.835 ± 0.048	0.819 ± 0.041	0.806 ± 0.034
Mean	0.894 ± 0.043	0.887 ± 0.042	0.880 ± 0.041
SD	0.063 ± 0.018	0.071 ± 0.020	0.076 ± 0.022

TABLE II
AUC FOR XDAWN+LDA CLASSIFICATION.

Subject	Mag	Grad	All
s1	0.943 ± 0.032	0.941 ± 0.033	0.942 ± 0.027
s2	0.869 ± 0.066	0.870 ± 0.070	0.859 ± 0.073
s3	0.813 ± 0.042	0.797 ± 0.034	0.783 ± 0.025
Mean	0.875 ± 0.047	0.869 ± 0.045	0.861 ± 0.042
SD	0.065 ± 0.017	0.072 ± 0.021	0.079 ± 0.027

IV. DISCUSSION

Despite the current requirements for technologies such as MEG and fMRI in term of cost and space, it is highly anticipated that those devices will become portable and smaller in a near future, following the same evolution of EEG amplifier devices. For this reason, MEG based BMI systems stay relevant thanks to the quality of the signal obtained by the high time and space resolution. Whereas the size of the device can be an issue for BMI that are used at home for

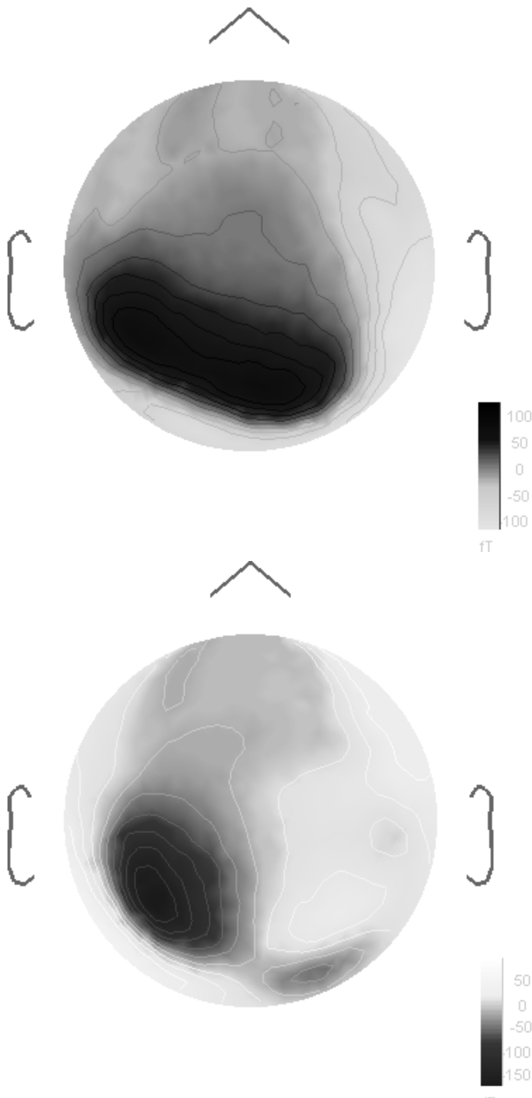

Fig. 4. Spatial distribution corresponding to the difference between targets and non-target at 200 ms (**top**) and 350 ms (**bottom**).

TABLE III
AUC FOR XDAWN+KNN (K=5) CLASSIFICATION.

Subject	Mag	Grad	All
s1	0.896 ± 0.052	0.899 ± 0.063	0.890 ± 0.056
s2	0.781 ± 0.101	0.762 ± 0.117	0.770 ± 0.116
s3	0.703 ± 0.051	0.697 ± 0.053	0.683 ± 0.055
Mean	0.793 ± 0.068	0.786 ± 0.077	0.781 ± 0.075
SD	0.097 ± 0.029	0.103 ± 0.035	0.104 ± 0.035

TABLE IV
AUC FOR XDAWN+SVM CLASSIFICATION.

Subject	Mag	Grad	All
s1	0.941 ± 0.013	0.938 ± 0.018	0.924 ± 0.015
s2	0.601 ± 0.135	0.571 ± 0.164	0.645 ± 0.190
s3	0.501 ± 0.015	0.523 ± 0.039	0.536 ± 0.008
Mean	0.681 ± 0.054	0.678 ± 0.073	0.702 ± 0.071
SD	0.231 ± 0.070	0.227 ± 0.079	0.201 ± 0.104

patient rehabilitation, MEG signal can probably significantly improve the quality of therapy sessions using neurofeedback thanks to the definition of more precise sources. Indeed, it may be judicious to have shorter session with a patient using an MEG based system, than long sessions with a portable EEG system. Brain recording devices have been mainly used for clinical applications. Yet, BMI can be advantageously exploited for military applications [40], where the performance, the accuracy of the decision is the main goal. In addition, for target-detection systems based on the detection of brain responses, the size of the signal recording device may not be an issue.

In the presented study, the images in the RSVP task were realistic images with no control on the contrast or the color. The characters were always placed at the fixation point but in various angles, and under different shades. Because the images for both the target and non-target classes contained objects that are contextually inconsistent, it can be assumed that the task was more difficult than the detection of more simpler objects (*e.g.,* geometric shapes). With the high number of channels, the number of trials may not have been high enough to train the classifier, and to estimate the spatial filters. Moreover, the spatial filters were only estimated on a large time segment. The estimation of spatial filters on different time segments may provide better results.

The current classification task did only involve two categories of images. Since novel images may be processed and be visually close to the target images, it would impair the performance. If the categories of images are very close, then the difficulty of the task increases, and the subject has to find a feature that will allow him to discriminate between the two classes. This new feature may have an impact on the characteristics of the brain evoked response. This is why incremental solutions should be implemented to track potential changes of the problem over time (the images become too noisy, the difficulty of the task changes).

V. CONCLUSION

In this paper, we have shown that it is possible to achieve high performance for single-trial detection of brain responses corresponding to the presentation of images during a rapid serial visual presentation task. The performance with magneto-meters was relatively similar to the performance using gradio-meters. Hence, this study suggests that only 102 channels could be enough to perform robust single-trial detection. Different approaches should be investigated to better take into account unique brain patterns that can be found with the gradio-meters. Future works will include the addition of other classes of images to go beyond binary single-trial detection.

Acknowledgment

The authors would like to thank the NI Functional Brain Mapping Facility project (1303/101154803) funded by InvestNI and Ulster University. The authors would like to thank Richard Gault and Jose Miguel Sanchez Bornot for their help during the experiments.

References

[1] M. Hämäläinen, R. Hari, R. J. Ilmoniemi, J. Knuutila, and O. V. Lounasmaa, "Magnetoencephalography: theory, instrumentation, and applications to noninvasive studies of the working human brain," *Rev. Mod. Phys.*, vol. 65, no. 2, pp. 413–497, Apr. 1993.

[2] Y. Kamitani and F. Tong, "Decoding the visual and subjective contents of the human brain," *Nature Neuroscience*, vol. 8, no. 5, pp. 679–685, 2005.

[3] K. N. Kay, T. Naselaris, R. J. Prenger, and J. L. Gallant, "Identifying natural images from human brain activity," *Nature*, vol. 452, no. 20, pp. 352–355, 2008.

[4] J. Wang, E. Pohlmeyer, B. Hanna, Y.-G. Jiang, P. Sajda, and S.-F. Chang, "Brain state decoding for rapid image retrieval," in *Proc. of the 17th ACM international conference on Multimedia*, 2009, pp. 945–954.

[5] Y. Miyawaki, H. Uchida, O. Yamashita, M. A. Sato, Y. Morito, H. C. Tanabe, N. Sadato, and Y. Kamitani, "Visual image reconstruction from human brain activity using a combination of multiscale local image decoders," *Neuron*, vol. 60, no. 5, pp. 915–929, 2008.

[6] J. R. Wolpaw, N. Birbaumer, D. J. McFarland, G. Pfurtscheller, and T. M. Vaughan, "Brain-computer interfaces for communication and control," *Clin Neurophysiol*, vol. 113, pp. 767–791, 2002.

[7] L. Farwell and E. Donchin, "Talking off the top of your head: toward a mental prosthesis utilizing event-related brain potentials," *Electroencephalogr. Clin. Neurophysiol.*, vol. 70, pp. 510–523, 1988.

[8] B. Hong, F. Guo, T. Liu, X. Gao, and S. Gao, "N200-speller using motion-onset visual response," *Clinicial Neurophysiology*, vol. 120, pp. 1658–1666, 2009.

[9] A. Rakotomamonjy and V. Guigue, "BCI competition iii : Dataset ii - ensemble of SVMs for BCI P300 speller," *IEEE Trans. Biomedical Engineering*, vol. 55, no. 3, pp. 1147–1154, 2008.

[10] H. Cecotti, "Spelling with non-invasive brain-computer interfaces - current and future trends," *J. Physiology-Paris*, vol. 105, no. 1-3, pp. 106–114, 2011.

[11] ——, "Toward shift invariant detection of event-related potentials in non-invasive brain-computer interface," *Pattern Recognition Letters (in press)*, in press.

[12] P. Sajda, A. Gerson, and L. Parra, "High-throughput image search via single-trial event detection in a rapid serial visual presentation task," *In Proc. of the 1st Int. IEEE EMBS Conf. Neural Eng.*, pp. 7–10, 2003.

[13] Y. Huang, D. Erdogmus, M. Pavel, S. Mathan, and K. E. Hild, "A framework for visual image search using single-trial brain responses," *Neurocomputing*, vol. 74, pp. 2041–2051, 2011.

[14] M. C. Potter, "Short-term conceptual memory for pictures," *Journal of Experimental Psychology: Human Learning and Memory*, vol. 2, pp. 509–522, 1976.

[15] M. M. Chun and C. M. Potter, "A two-stage model for multiple target detection in rapid serial visual presentation," *J. Exp. Psy. Human Perception and Performance*, vol. 21, no. 1, pp. 109–127, 1995.

[16] N. Bigdely-Shamlo, A. Vankov, R. R. Ramirez, and S. Makeig, "Brain activity-based image classification from rapid serial visual presentation," *IEEE Trans. on Neural Systems and Rehab. Eng.*, vol. 16, no. 5, pp. 432–41, 2008.

[17] A. Gerson, L. Parra, and P. Sajda, "Cortically-coupled computer vision for rapid image search," *IEEE Trans. Neural Syst. Rehabil. Eng.*, vol. 14, no. 2, pp. 174–179, 2006.

[18] L. C. Parra, C. Christoforou, A. D. Gerson, M. Dyrholm, A. Luo, M. Wagner, M. G. Philiastides, and P. Sajda, "Spatio-temporal linear decoding of brain state: Application to performance augmentation in high-throughput tasks," *IEEE Signal Process. Mag.*, vol. 25, no. 1, pp. 95–115, 2008.

[19] E. A. Pohlmeyer, D. C. Jangraw, J. Wang, S. F. Chang, and P. Sajda, "Combining computer and human vision into a BCI: can the whole be greater than the sum of its parts?" *32nd International IEEE EMBC Conference*, pp. 138–41, 2010.

[20] E. A. Pohlmeyer, J. Wang, D. C. Jangraw, B. Lou, S. Chang, and P. Sajda, "Closing the loop in cortically-coupled computer vision: a brain-computer interface for searching image databases," *J. Neural Eng.*, vol. 8, p. 036025, 2011.

[21] J. Touryan, L. Gibson, H. J. Horne, and P. Weber, "Real-time measurement of face recognition in rapid serial visual representation," *Frontiers in Psychology*, vol. 2, no. 42, pp. 1–8, 2011.

[22] K. E. Hild, M. Kurimo, and V. D. Calhoun, "The sixth annual MLSP competition, 2010," *IEEE International Workshop on Machine Learning for Signal Processing (MLSP)*, pp. 107–111, 2010.

[23] T. Fawcett, "An introduction to ROC analysis," *Pattern Recognition Letters*, vol. 27, pp. 861–874, 2006.

[24] L. Parra, C. Alvino, A. Tang, B. Pearlmutter, N. Yeung, A. Osman, and P. Sajda, "Single trial detection in EEG and MEG: Keeping it linear," *Neurocomputing*, vol. 52-54, pp. 177–183, 2003.

[25] U. Hoffmann, J. Vesin, K. Diserens, and T. Ebrahimi, "An efficient P300-based brain-computer interface for disabled subjects," *Journal of Neuroscience Methods*, vol. 167, no. 1, pp. 115–125, 2008.

[26] H. Cecotti, A. Ries, M. Eckstein, and B. Giesbrecht, "Multiclass classification of single trial evoked eeg responses," in *Proc. of the 34nd Int. IEEE EMBC*, 2012, pp. 1719–22.

[27] H. Cecotti and A. Gräser, "Convolutional neural networks for P300 detection with application to brain-computer interfaces," *IEEE Trans. Pattern Analysis and Machine Intelligence*, vol. 33, no. 3, pp. 433–445, Mar. 2011.

[28] H. Cecotti, M. P. Eckstein, and B. Giesbrecht, "Single-trial classification of event-related potentials in rapid serial visual presentation tasks using supervised spatial filtering," *IEEE Trans. Neural Networks and Learning Systems*, vol. 15, pp. 2030–42, Nov. 2014.

[29] H. Cecotti, J. Sato-Reinhold, J. Sy, J. Elliott, M. Eckstein, and B. Giesbrecht, "Impact of target probability on single-trial eeg target detection in a difficult rapid serial visual presentation task," in *Proc. of the 33nd Int. IEEE EMBC*, 2011, pp. 6381–4.

[30] S. Taulu, J. Simola, and M. Kajola, "Applications of the signal space separation method," *IEEE Trans. Signal Processing*, vol. 53, no. 9, Sept. 2005.

[31] S. Taulu and M. Kajola, "Presentation of electromagnetic multichannel data: the signal space separation method," *Journal of Applied Physics*, vol. 97, p. 124905, 2005.

[32] S. Taulu and J. Simola, "Spatiotemporal signal space separation method for rejecting nearby interference in meg measurements," *Phys. Med. Biol.*, vol. 51, pp. 1–10, 2006.

[33] B. Rivet, A. Souloumiac, V. Attina, and G. Gibert, "xDAWN algorithm to enhance evoked potentials: application to brain-computer interface," *IEEE Trans Biomed. Eng.*, vol. 56, no. 8, pp. 2035–43, 2009.

[34] B. Rivet, H. Cecotti, R. Phlypo, O. Bertrand, E. Maby, and J. Mattout, "Eeg sensor selection by sparse spatial filtering in p300 speller brain-computer interface," in *Proc. of the 32nd International IEEE Conference of the Engineering in Medicine and Biology Society*, 2010, pp. 5379–82.

[35] H. Cecotti, B. Rivet, M. Congedo, C. Jutten, O. Bertrand, E. Maby, and J. Mattout, "A robust sensor selection method for P300 brain-computer interfaces," *J. Neural Eng.*, vol. 8, p. 016001, 2011.

[36] B. Rivet, H. Cecotti, E. Maby, and J. Mattout, "Impact of spatial filters during sensor selection in a visual P300 brain-computer interface," *Brain Topography*, vol. 12, no. 1, pp. 55–63, 2012.

[37] B. Rivet and A. Souloumiac, "Optimal linear spatial filters for event-related potentials based on a spatio-temporal model: Asymptotical performance analysis," *Signal Processing*, vol. 93, no. 2, pp. 387–398, 2013.

[38] F. Tadel, S. Baillet, J. C. Mosher, D. Pantazis, and R. M. Leahy, "Brainstorm: A user-friendly application for meg/eeg analysis," *Computational Intelligence and Neuroscience*, vol. 2011, no. 879716, pp. 1–13, 2011.

[39] J. Polich, "Updating P300: An integrative theory of P3a and P3b," *Clinical Neurophysiology*, vol. 118, pp. 2128–2148, 2007.

[40] R. A. Miranda, W. D. Casebeer, A. M. Hein, J. W. Judy, E. P. Krotkov, T. L. Laabs, J. E. Manzo, K. G. Pankratz, G. A. Pratt, J. C. Sanchez, D. J. Weber, T. L. Wheeler, and G. S. F. Ling, "Darpa-funded efforts in the development of novel braincomputer interface technologies," *J. of Neuroscience Methods*, 2014.